ELSEVIER

Journal of Pharmaceutical and Biomedical Analysis
16 (1997) 661–673

JOURNAL OF
PHARMACEUTICAL
AND BIOMEDICAL
ANALYSIS

Spectroscopic identification of an amorphous-to-crystalline drug transition in a solid dispersion SCH 48461 capsule formulation

Robert J. Markovich *, C. Anderson Evans, Corazon B. Coscolluela, Sigita A. Zibas, Jack Rosen

Department of Physical and Analytical Chemistry Research and Development, Schering-Plough Research Institute, 2000 Galloping Hill Road, Kenilworth, NJ 07033, USA

Received 1 November 1996; received in revised form 23 February 1997

Abstract

Changes in the dissolution of a solid dispersion capsule formulation composed of amorphous SCH 48461 in a polyethylene glycol 8000 matrix were investigated. SCH 48461 [(3*R*,4*S*)-1,4-bis(4-methoxyphenyl)-3-(3-phenylpropyl)-2-azetidinone] is a potent cholesterol absorption inhibitor with low water solubility and low melting point. Several capsule lots placed under controlled storage conditions exhibited a slowing of dissolution as a function of time with large inter-lot and intra-lot dissolution variations. Capsule contents were analyzed by attenuated total reflectance infrared (ATR-IR) microspectroscopy and solid-state cross-polarization, magic angle spinning (CPMAS) ^{13}C-nuclear magnetic resonance (NMR) spectrometry. ATR-IR microspectroscopic analysis showed large IR spectral differences between the lots including the presence of a crystalline drug fraction in lots which exhibited incomplete dissolution. Solid-state CPMAS ^{13}C-NMR analysis confirmed the presence of a crystalline drug fraction in the problematic capsule lots. Both ATR-IR and CPMAS ^{13}C-NMR spectral results produced a rank ordering of the crystalline drug fraction present in the capsule lots that correspond to the dissolution results. © 1997 Elsevier Science B.V.

Keywords: Attenuated total reflectance infrared (ATR-IR) microspectroscopy; Crystalline and amorphous drug; Dissolution; SCH 48461; Solid dispersion

1. Introduction

The solid-state form (i.e., crystalline polymorphs, solvates, amorphous solids) of a drug substance can have a significant impact on the drug's solubility, dissolution rate, stability in a pharmaceutical formulation, and bioavailability [1,2]. Although the amorphous solids are often susceptible to changes during storage, the amorphous form of a drug is generally more soluble, which is a useful property particularly if the drug has low aqueous solubility [2,3]. Formulation techniques have been developed to increase the bioavailability and aqueous dissolution of poorly water-soluble drug by simultaneously reducing drug particle size and altering the drug crystal form [2,4]. One such technique is called solid

* Corresponding author. Tel.: +1 908 2982453; fax: +1 908 2982107; e-mail: robert.markovich@spcorp.com.

PII S0731-7085(97)00083-6

dispersion which is a dispersion of the drug (in the desired solid-state form) in an inert carrier matrix prepared by the melting (fusion), solvent, or melting–solvent method [2,4].

The melt (fusion) solid dispersion formulation technique was used for the manufacture of SCH 48461 capsules. SCH 48461 [(3*R*,4*S*)-1,4-bis(4-methoxyphenyl)-3-(3-phenylpropyl)-2-azetidinone] is a potent cholesterol absorption inhibitor [5,6] with low water solubility (< 0.0001 mg ml^{-1}) and low melting point (about 40–42°C). The structure of this compound and crystallographic atom numbering scheme are shown in Fig. 1. The solid dispersion capsules, which contain 200 mg of drug (625 mg total capsule content weight), were produced by melting the drug–polyethylene glycol (PEG) 8000 mixture in a 1:2 ratio at 70°C and liquid-filling gelatin capsules with the liquid melt. The liquid melt capsule filling technique has been previously described [7]. The liquid melt inside the capsule solidifies at room temperature to form a solid, waxy capsule core. Several capsule lots placed under controlled storage conditions exhibited a slowing of dissolution as a function of time with large inter-lot and intra-lot dissolution variations. These varying dissolution results occurred even though drug content uniformity and assay results were 100% of the labeled strength. In addition, X-ray powder diffraction analysis of the capsule contents failed to show any initial lot-to-lot differences and no change from the initial diffraction pattern as a function of time and storage condition. This study's objective was to identify the cause of the changing dissolution characteristics of the SCH 48461 capsule lots.

2. Materials and methods

2.1. Materials

Sodium lauryl sulfate, 99% especially pure grade, was purchased from BDH Laboratories (Poole, UK). Polyethylene glycol 8000 NF grade was purchased from Union Carbide Corporation (Charleston, WV). White Opaque ELC capsules No.0 were purchased from Shionogi Qualicaps (Indianapolis, IN). Hydrochloric acid reagent grade was purchased from Fisher Scientific (Fair Lawn, NJ). Adamantane was purchased from Aldrich Chemical Co. (Milwaukee, WI). The SCH 48461 capsules, 200 mg (625 mg total capsule content weight) were manufactured at Schering-Plough, Kenilworth, NJ. Storage conditions were 25°C/60% relative humidity (RH), 30°C/60% RH and 40°C/80% RH, and testing was performed at Schering-Plough Research Institute, Kenilworth, NJ.

2.2. Dissolution

The USP basket Apparatus 1 method (Vanderkamp VK6000 dissolution tester, Van-Kel Industries, Edison, NJ) was used to determine the dissolution rate in 1000 ml of 1% aqueous sodium lauryl sulfate (SLS) media at 100 rpm maintained at 37°C. Ultraviolet (UV) analysis (HP 8450, Hewlett Packard) was performed on the resulting filtered aliquots using a 0.1 cm cell and monitoring at 259 nm.

2.3. X-ray powder diffraction (XRD)

The solid, waxy SCH 48461 capsule contents were carefully ground/mashed prior to analysis. Powder X-ray diffraction patterns were obtained using a Philips model APD 3720 Automated Powder Diffraction System, equipped with a vertical

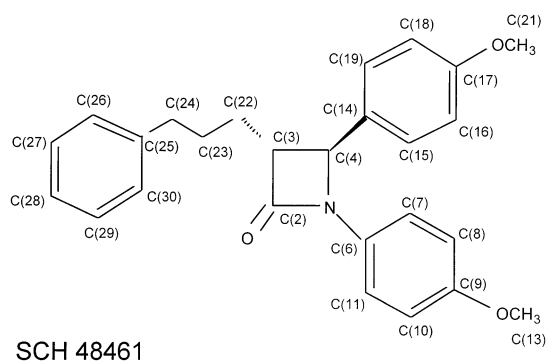

Fig. 1. The structure and crystallographic atom numbering scheme for SCH 48461 [(3*R*,4*S*)-1,4-bis(4-methoxyphenyl)-3-(3-phenylpropyl)-2-azetidinone].

goniometer with a take-off angle of 6° 2Ø, an automatic divergence slit, and a 0.2 mm receiving slit. A graphite monochromator and a scintillation detector were used. The X-ray generator (Philips model XRG 3100) was operated at 45 kV and 40 mA, using the Kα lines of copper at 1.54060 and 1.54439° as the radiation source. Each sample was scanned between 4 and 25° 2Ø at a scan rate of 0.025° s^{-1} using 0.010° step size.

2.4. Attenuated total reflectance infrared (ATR-IR) microspectroscopy

ATR-IR spectroscopy was performed on a Nicolet Magna-IR™ 550 series FTIR spectrometer with OMNIC™ software, Nic-Plan™ microscope with an ATR objective (ZnSe crystal), and an MCT-A liquid nitrogen cooled detector (detection range 4000–650 cm^{-1}). Spectra were obtained at 8 cm^{-1} resolution through a 1.5 mm aperture and the spectra were not smoothed. Interferograms from 128 scans were coadded with one level of zero filling and apodized with a Happ-Genzel function before Fourier transformation. Spectra were baseline corrected by drawing a line at three points (at approximately 650, 2000 and 4000 cm^{-1}). Each spectrum was obtained by making optical contact between the small spherical ATR crystal and approximately a 200 μM diameter circle of the capsule core surface. Each capsule was analyzed by first removing the capsule shell to expose the capsule core, obtaining an infrared spectrum of the core surface at two locations, slicing the capsule core in half lengthwise with a razor blade to expose the interior, and then obtaining an infrared spectrum of the capsule core interior at two locations.

2.5. Solid-state ^{13}C-nuclear magnetic resonance (NMR) spectroscopy

Solid-state ^{13}C-NMR spectroscopy was performed on a modified General Electric Model GN-300 FT-NMR Spectrometer equipped with a Doty Scientific 7 mm magic angle sample spinning (MASS) probe. Spectra were obtained at 75.47 MHz for carbon and high power proton decoupling at 300.1 MHz was performed during all acquisition times. Capsule cores samples (approximately 150 mg or 1/3 of total weight) were packed in 7 mm single crystal sapphire rotors with Kel-F® end-caps. Each capsule core was shaved slightly to fit in the sapphire rotor (both the shaved core and its shavings were analyzed and found to give identical results). NMR analysis were recorded with high power proton decoupling (55 kHz) and MASS at speeds of 5 kHz. Adamantane was used as an external chemical shift reference ($\delta = 38.453$ relative to tetramethylsilane (TMS)) for ^{13}C-NMR. The cross-polarization, magic angle spinning (CPMAS) pulse sequence was used to acquire the ^{13}C-NMR spectra. Each spectrum was acquired using an 8 K data set, spectral width of 50 000 Hz (corresponding to a dwell time of 20 μs), 1 or 2 s recycle time, 1 ms contact time, and 4.5 μs pulse width. Cross-depolarization (CDP) experiments used a 40 μs phase inversion time and the phase of the ^{1}H spin lock changed by 180° at the end of the contact time.

3. Results and discussion

The SCH 48461:PEG 8000 melt solid dispersion can be classified as an interstitial solid solution (i.e., the drug molecules occupy the interstitial space of the PEG 8000 crystal lattice) [2,4]. High molecular weight polyethylene glycols (4000 and higher) contain two parallel helixes per unit cell and significant amount of drug can be trapped in the helical interstitial space [4]. Many drug–PEG systems have been studied, most notably griseofulvin–PEG and indomethacin–PEG solid dispersion systems [2,4,8,9]. It has been reported that aging amorphous indomethacin–PEG and amorphous griseofulvin–PEG solid dispersions resulted in the formation of crystalline drug over time, which was dependent on both the drug–PEG ratio and storage conditions [8,9]. Furthermore, the amorphous-to-crystalline transition during aging of the indomethacin–PEG solid dispersion resulted in the significant reduction of indomethacin dissolution rates [8]. It has been suggested that solid dispersions may form amorphous deposits of drug by diffusional processes that can crystallize during storage [2,4,8,9]. Such

was the case for the SCH 48461–PEG solid dispersion system as identified by Fourier transform infrared (FT-IR) spectroscopy and NMR spectroscopy.

Methods used to characterize the solid-state form of a drug include X-ray powder diffraction, microscopy, thermal analysis, FT-IR spectroscopy and NMR spectroscopy [1]. X-ray powder diffraction is frequently the method of choice [1,3,10,11]. However, if the crystal is too small (10^{-5} cm or less) or in a distorted lattice then a diffuse diffraction pattern will occur [1,10]. Amorphous and crystal forms of a drug have nonequivalent spatial relationships that often result in different functional group vibrational modes (IR) and different nuclear resonance frequencies (NMR). Thus, FT-IR spectroscopy and NMR spectrometry can be used to monitor such drug solid-state form changes [12–22]. FT-IR and NMR solid-state analytical techniques are especially useful because they are nondestructive and typically require little or no sample preparation, thus the formulated product can be analyzed as received.

The SCH 48461 capsule lots were analyzed by attenuated total reflectance infrared (ATR-IR) microspectroscopy [23–28] and cross-polarization, magic angle spinning (CPMAS) solid-state ^{13}C-NMR spectrometry [1,29–34]. The spectral characteristics of the capsule contents were directly related to their dissolution profiles. Examination of the IR spectra suggested the presence of a crystalline drug fraction in the slow dissolving capsule lots. Solid-state CPMAS ^{13}C-NMR analysis confirmed the presence of crystalline drug fraction in the problematic capsule lots. Both ATR-IR and CPMAS ^{13}C-NMR spectral results produced a rank ordering of the crystalline drug fraction present in the capsule lots that correspond to the dissolution results.

3.1. Dissolution analysis

Crystalline SCH 48461 is poorly soluble in acidic or neutral aqueous media (<0.0001 mg ml^{-1}) and has limited solubility in 1% aqueous sodium lauryl sulfate (SLS, 0.022 mg ml^{-1}). However, by formulating 200 mg of SCH 48461 as a solid dispersion in 400 mg of PEG 8000 (1:2 ratio), complete drug release was achieved in 1000 ml of 1% SLS within 60 min. Based on the dissolution behavior of the capsule product (at least 0.2 mg ml^{-1} solubility required), at least a 10-fold increase in drug solubility was realized by formulating SCH 48461 capsules as a drug:PEG 8000 solid dispersion.

The differences in the relative dissolution rates and changes in dissolution during stability test conditions for lots A, B and C are illustrated in Fig. 2(a)–(c). Fig. 2(a) compares the dissolution rate profiles shortly after manufacture (i.e., initial time point). These dissolution rate profiles clearly show that initially lot C is significantly different from lots A and B. Lot B, placed under controlled storage conditions for 18 months, exhibited a slowing of dissolution over time (Fig. 2(b)) and large intra-lot variations of individual capsule dissolution profiles (Fig. 2(c)).

3.2. X-ray powder diffraction analysis

X-ray powder diffraction (XRD) analysis was performed at the initial time point and throughout the stability program for lots A, B and C. X-ray powder diffraction analysis of all sample lots indicated only the presence of amorphous drug at the initial stability timepoint and no change from the initial diffraction pattern as a function of time and storage condition. Fig. 3 shows the X-ray diffraction patterns of (a) SCH 48461 capsule lot C, (b) PEG 8000 and (c) crystalline SCH 48461 drug, and clearly demonstrates that XRD does not detect crystalline SCH 48461 in lot C. The diffraction pattern of lot C is typical of all SCH 48461 capsule lots tested and thus XRD analysis was unable to differentiate between the lots having fast dissolution profiles (lot A) or slow/incomplete dissolution profiles (lots B and C). One definition of an amorphous solid is a solid material whose particle size is too small to yield a measurable powder pattern; this definition allows for the existence of order without specifying how far the order extends[1]. Although XRD failed to indicate the presence of crystalline drug,

[1] We are grateful to the reviewer for providing this alternate definition of an amorphous solid.

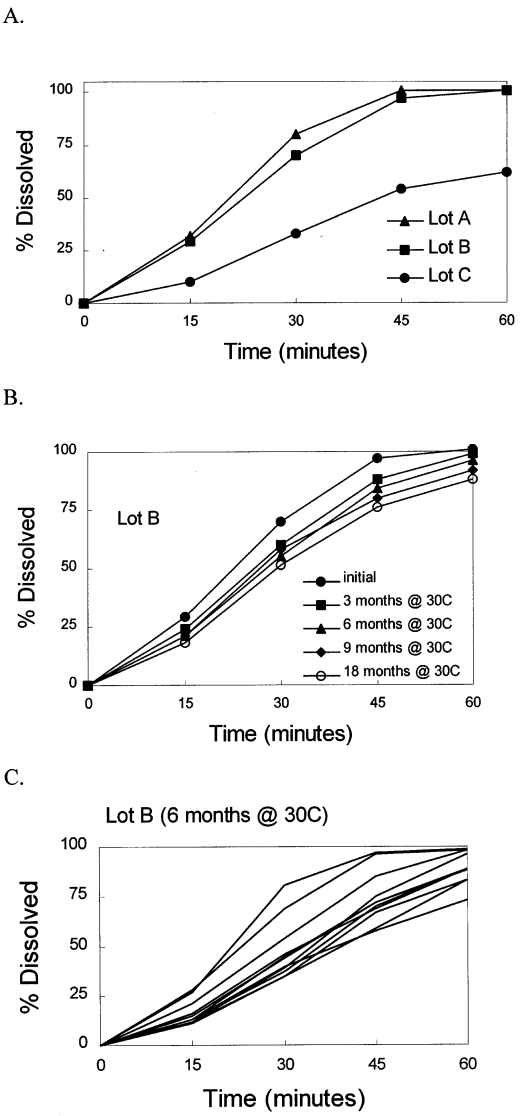

Fig. 2. The differences in the dissolution rate profiles: (a) as a function of lot for SCH 48461 capsule lots A, B and C shortly after manufacture (i.e., initial time point); (b) as a function of stability for SCH 48461 capsule lot B over 18 months stored at 30°C/60% relative humidity (RH); and (c) within a stability timepoint for SCH 48461 capsule lot B (6 months at 30°C/60% RH).

crystalline (or ordered amorphous) drug may be present in such a way that it is below the detection limit of XRD. XRD lines become diffuse when crystal sizes fall below 10^{-5} cm, which is still above the atomic dimension limit of 10^{-8} cm [1,4]. Furthermore, samples which generate relatively diffuse diffraction patterns can have one- or two-dimensional degrees of order and even three-dimensional order with severe lattice distortions [4]. Thus FT-IR spectroscopy and solid-state ^{13}C-NMR spectrometry were used to investigate the differences between SCH 48461 capsule lots.

3.3. Infrared analysis

Infrared analysis was performed using ATR-IR microspectroscopy [23–28]. This allowed the direct (in-situ) analysis of highly absorbing materials without compromising the sample (i.e., KBr pellets, etc.) and provides a fixed reproducible pathlength for accurate qualitative/quantitative information [27,28]. The small spherical ATR crystal located on the objective of an IR microscope is placed on the capsule core, optical contact is made between the sample surface of interest and the ATR crystal, and an infrared spectrum is obtained. This technique produced a series of localized IR spectra of an individual capsule core samples.

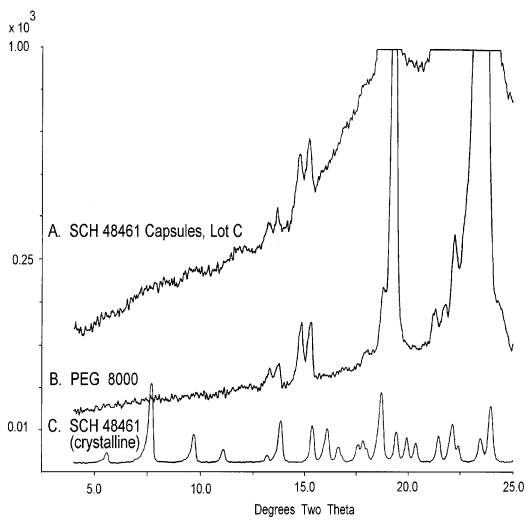

Fig. 3. The X-ray powder diffraction patterns of (a) the capsule core matrix of SCH 48461 capsule lot C (15 months at room temperature), (b) the excipient PEG 8000, and (c) crystalline SCH 48461 drug.

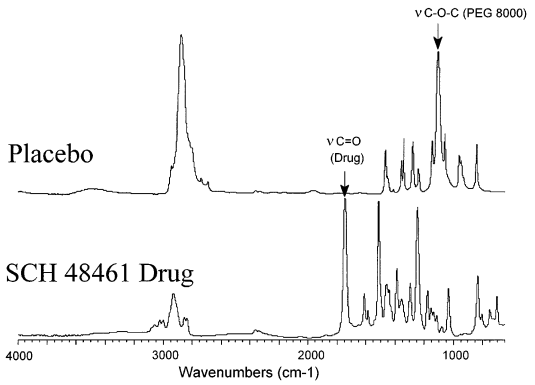

Fig. 4. The ATR-IR spectra of the SCH 48461 placebo capsule matrix and amorphous SCH 48461 drug substance. The IR bands arising from the PEG 8000 ether (νC–O–C) group at approximately 1100 cm^{-1} and from the SCH 48461 drug lactam carbonyl (νC=O) group at approximately 1740 cm^{-1} are identified.

The comparison of infrared spectra of the placebo matrix and drug substance (amorphous form) is shown in Fig. 4. The placebo matrix spectrum (Fig. 4, top) contains an intense ether (νC–O–C) group IR band at approximately 1100 cm^{-1} from PEG 8000 in a region where there is insignificant interference from the SCH 48461 drug spectrum. The SCH 48461 drug spectrum (Fig. 4, bottom) contains an intense lactam carbonyl (νC=O) group IR band at approximately 1740 cm^{-1} in a region where there are no interfering bands from the placebo matrix spectrum. A rapid screening technique was developed by monitoring the drug/PEG 8000 IR peak height ratio (absorbance νC=O/absorbance νC–O–C) of the SCH 48461 capsule lots. Any differences between the sample spectra (i.e., peak location, peak shape and relative peak intensities) may help identify the source of the capsule lot differences as identified by the dissolution profiles.

Fig. 5(a) and (b) illustrate that lots A and C have very different ATR-IR capsule core spectra and different drug/PEG 8000 IR peak height ratios. Fig. 5(a) shows a representative spectrum from lot A and the corresponding drug/PEG 8000 IR peak height ratio (absorbance νC=O/absorbance νC–O–C = 0.40). Fig. 5(b) shows a representative spectrum from lot C and the corresponding drug/PEG 8000 IR peak height ratio (absorbance νC=O/absorbance νC–O–C = 1.16). The drug/PEG 8000 IR peak height ratio data for lot A (Table 1, top) indicated little or no inter- and intra-capsule spectral differences. In contrast, the drug/PEG 8000 IR peak height ratio data for lot C (Table 1, bottom) indicated very large inter- and intra-capsule spectral differences. Finally, the drug/PEG 8000 IR peak height ratios for lot B (Table 2) indicated that lot B had infrared spectral characteristics somewhere between lot A and lot C.

The IR spectral differences between lots A, B and C led to further examination of the drug substance infrared spectrum. The spectra of the crystalline and amorphous forms of SCH 48461

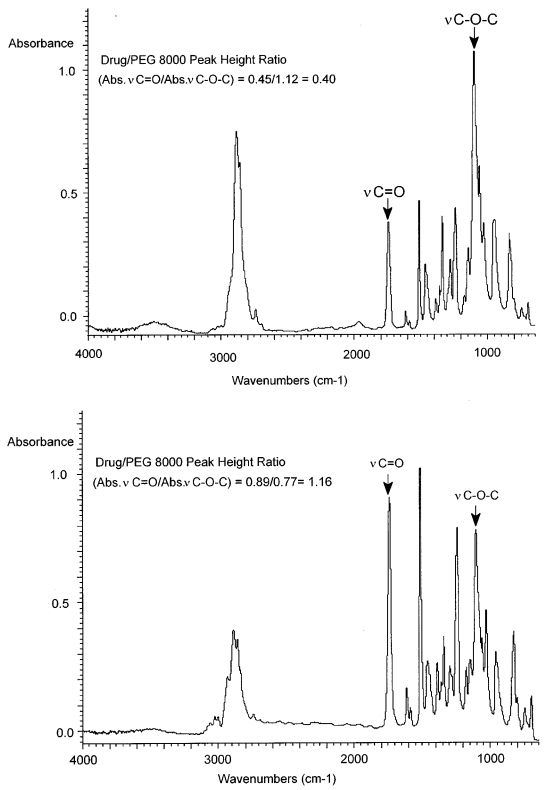

Fig. 5. The ATR-IR spectra of representative capsule cores from (a) SCH 48461 capsule lot A and (b) SCH 48461 capsule lot C. The calculation of the drug/PEG 8000 IR peak height ratio (absorbance νC=O/absorbance νC–O–C) is indicated for each spectrum.

Table 1
The drug/PEG 8000 IR peak height ratio data generated from the ATR-IR spectra from the capsule cores of SCH 48461 capsule lot A (at initial) and lot C (13 months at room temperature)

Capsule region	Avg	High	Low	Peak height ratio (SCH 48461 active/PEG 8000 (absorbance νC=O/absorbance νC–O–C)[a]					
				1	2	3	4	5	6
Lot A (initial)									
Core surface	0.35	0.40	0.28	0.39	0.35	0.33	0.39	0.35	0.33
				0.35	0.34	0.35	0.28	0.40	0.37
Core interior	0.40	0.49	0.31	0.43	0.44	0.31	0.39	0.36	0.40
				0.38	0.44	0.49	0.32	0.43	0.39
Lot C (13 months at room temperature)									
Core surface	0.78	1.16	0.32	1.16	1.12	0.65	0.82	0.56	0.72
				0.82	0.89	0.96	0.72	0.32	0.60
									0.78
Core interior	0.58	1.48	0.22	0.40	0.35	1.05	0.35	0.72	0.22
				0.23	0.64	1.48	0.56	0.44	0.24
								0.82	

At least four spectra per capsule core were obtained, two on the capsule core surface and two on the capsule core interior.
[a] The IR band at approximately 1740 cm^{-1} is the νC=O stretching vibration of the SCH 48461 active and the IR band at approximately 1100 cm^{-1} is the νO–C–O stretching vibration of PEG 8000.

are compared in Fig. 6(a) and (b). Although many infrared band differences exist between the crystalline and amorphous forms in the C–H stretching region (Fig. 6(a), 3100–2800 cm^{-1}), this region was not useful because of the interfering bands from the PEG 8000 (see Fig. 4). However, Fig. 6(b) shows that the spectral region from 2000 to 650 cm^{-1} is useful for the comparison of the crystalline and amorphous drug forms. Differences include: (a) lactam νC=O (amide I) peak shift from 1746 cm^{-1} (amorphous) to 1736 cm^{-1} (crystalline); (b) increased band intensities in the aromatic νC=C at 1620, 1590 and 1441 cm^{-1}; (c) increased band intensity of the lactam νC–N at 1179 cm^{-1}; (d) increased band intensity of the aromatic ν_{sy}C–O–C at 1035 cm^{-1}; and (e)–(g) increased band intensities in the aromatic δC–H out of plane bend (mono-substituted (e) 957, (f) 909, and (j) 750 cm^{-1}; di-substituted (g) 869, (h) 835, and (i) 803 cm^{-1}).

It should be recalled that X-ray powder diffraction analysis of all lot C samples indicated only the presence of amorphous drug and no changes in the diffraction pattern as a function of stability. Infrared spectral analysis of the same lot C samples revealed significant differences.

Fig. 7 compares four spectra obtained from capsule # 1 of lot C (refer to Table 1) with the resulting drug/PEG 8000 IR peak height ratios on the left of the figure. Note that as the drug/PEG 8000 peak height ratio increases, the infrared bands attributable to the drug substance begin to resemble that of crystalline SCH 48461 as noted by the bands identified by letters (a)–(j). This comparison suggests that as the drug/PEG 8000 peak height ratio increases, the amount of crystalline drug increases in the solid dispersion matrix. Similar comparisons were made for all capsules analyzed (not shown) and a rank ordering of the SCH 48461 capsule lots based on their IR spectral characteristics (i.e., relative peak ratios) was made. The results show that amount of crystallinity increases from lot A < lot B < lot C, which is directly correlated to their respective dissolution profiles (Fig. 2(a)–(c)).

3.4. Solid-state ^{13}C-NMR analysis

The presence, or absence, of the crystalline drug in the various SCH 48461 capsule lots was confi-

Table 2
The drug/PEG 8000 IR peak height ratio data generated from the ATR-IR spectra from the capsule cores of SCH 48461 capsule lot B stored for 13 months at 30°C, for 1 month at 40°C, and for 6 months at 40°C

Capsule region	Avg	High	Low	Peak height ratio (SCH 48461 active/PEG 8000) (absorbance νC=O/absorbance νC–O–C)[a]					
				1	2	3	4	5	6
Lot B (13 months at 30°C)									
Core surface	0.43	0.62	0.34	0.36	0.62	0.43	0.35	0.34	0.55
				0.35	0.42	0.50	0.44	0.39	0.46
Core interior	0.51	1.62	0.25	0.33	0.40	0.32	0.35	0.38	0.72
				0.25	0.69	0.32	0.31	0.36	0.47
					1.62				0.59
Lot B (1 month at 40°C)									
Core surface	0.44	0.65	0.31	0.32	0.32	0.55	0.41	0.51	0.35
				0.60	0.31	0.61	0.38	0.65	0.32
Core interior	0.47	0.64	0.38	0.52	0.52	0.48	0.39	0.64	0.43
				0.56	0.41	0.44	0.43	0.44	0.38
Lot B (6 months at 40°C)									
Core surface	0.43	0.67	0.28	0.30	0.34	0.47	0.41	0.37	0.57
				0.36	0.41	0.43	0.55	0.28	0.67
Core interior	0.51	0.86	0.36	0.38	0.50	0.58	0.60	0.36	0.54
				NT	0.86	0.51	0.45	0.46	0.41

At least four spectra per capsule core were obtained, two on the capsule core surface and two on the capsule core interior. NT, not tested.
[a] The IR band at approximately 1740 cm^{-1} is the νC=O stretching vibration of the SCH 48461 active and the IR band at approximately 1100 cm^{-1} is the νO–C–O stretching vibration of PEG 8000.

rmed by solid-state CPMAS ^{13}C-NMR spectrometry. This technique overcomes several problems encountered with classical solid-state ^{13}C-NMR by using strong proton decoupling (which eliminates neighboring nuclei interactions), rapidly spinning the sample tube at the magic angle of 54°44′ (which removes the effect of randomly oriented powders), and using the cross-polarization pulse sequence (which allows for faster acquisition of data) [34].

The CPMAS ^{13}C-NMR spectrum of the placebo matrix consists of a single broad peak at 70 ppm attributable to the PEG 8000 methylenes (not shown). The CPMAS ^{13}C-NMR spectrum of the drug substance (amorphous form) contains two broad peaks which are attributable to the aromatic carbons (120 ppm) and the terminal methoxy methyls (50 ppm) similar to that found in Fig. 8. Representative CPMAS ^{13}C-NMR spectra of intact capsule cores from lots A, B and C are shown in Figs. 8–10, respectively. The NMR peak assignments correspond to the structure and atom numbering scheme shown in Fig. 1. The important peak assignments in the lot C spectrum (Fig. 10, top) include the lactam ring carbonyl (C2), aryl C–Os (C17, C9), aryl C–N (C6), lactam ring methines (C3, C4), methoxy methyls (C13, C21), and the propyl methylenes (C22, C23, C24). The solid-state CPMAS ^{13}C-NMR peak assignments can be directly associated with the corresponding liquid state ^{13}C-NMR peak assignments (not shown). The CPMAS ^{13}C-NMR spectrum of lot C (Fig. 10, top) is in stark contrast to the spectra of lots A (Fig. 8) and B (Fig. 9). Amorphous materials generally give rise to relatively featureless CPMAS spectra, such as those observed for lots A and B in Figs. 8 and 9, because the drug molecules are randomly oriented with respect to each other. These spectra indicate that SCH 48461 molecules in lots A and B are in

an amorphous environment. The linewidths of these spectra are greater than would be expected for a randomly oriented solid. The additional linewidth can be explained by the presence of molecular motion at an intermediate rate which results in an incomplete averaging of the chemical shift tensor. The presence of molecular motion for these samples is also indicated by the slower rate at which the samples cross-polarize (see cross-polarization discussion below for lot C).

The narrow line CPMAS spectrum observed for lot C in Fig. 10 (top) can arise from only two sources: (1) the liquid-like character of plastic or waxy solids in rapid, large amplitude molecular motion; or (2) highly rigid, crystalline materials where the microenvironment of all the molecules are the same. These two narrow line possibilities can be distinguished by experiments that take advantage of properties of the proton-bearing carbons of the solid state. In these experiments, one of which is called cross-depolarization [32] and the other interrupted decoupling [33], the signal for the rigidly held (i.e., crystalline) ^{13}C having a directly bonded hydrogen will disappear (or possibly invert in the case of the cross-depolarization experiment).

Cross-depolarized or interrupted decoupled ^{13}C-NMR spectrum of a crystalline solid would contain peaks from only quaternary carbons (–C–) and methyl carbons ($-CH_3$). Quaternary car-

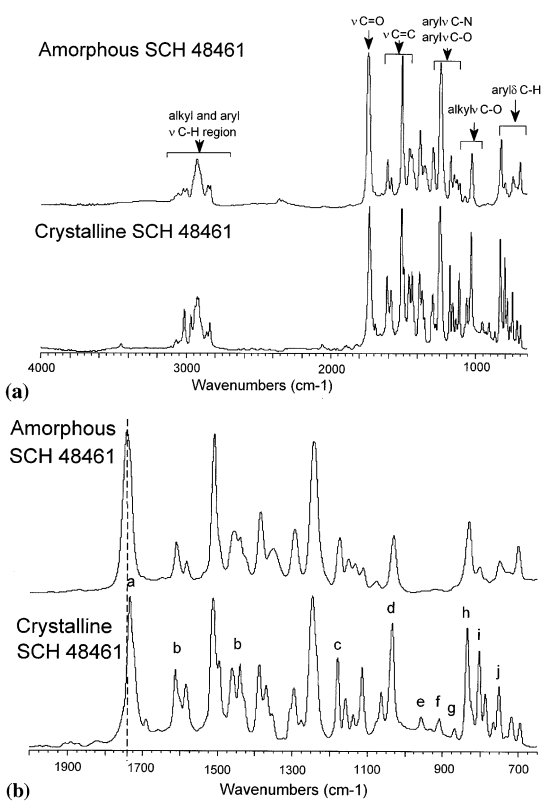

Fig. 6. The ATR-IR spectra of the two known forms of SCH 48461, crystalline and amorphous presented in the region: (a) from 4000 to 650 cm^{-1}; and (b) from 2000 to 650 cm^{-1}.

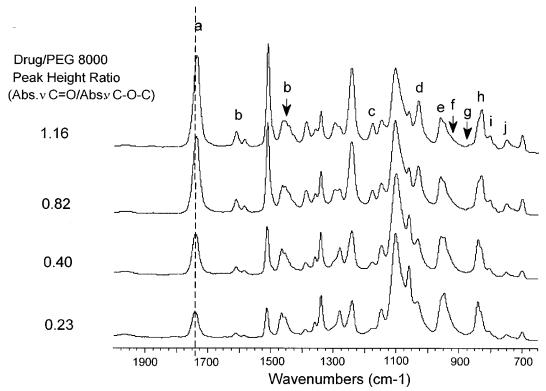

Fig. 7. Four ATR-IR spectra obtained from capsule # 1 in lot C (refer to Table 1) with the resulting drug/PEG 8000 IR peak height ratios on the left of the figure.

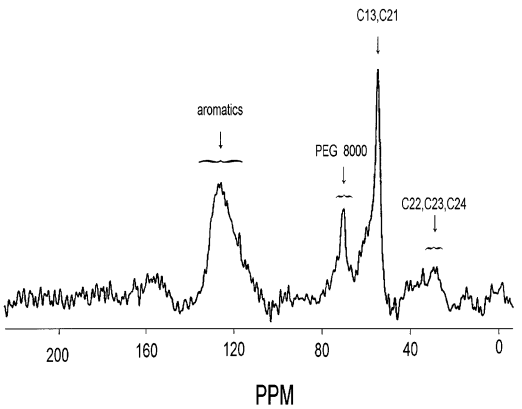

Fig. 8. The CPMAS ^{13}C-NMR spectrum of an intact capsule core from SCH 48461 capsule lot A (6 months at room temperature). The NMR peak assignments correspond to the structure and atom numbering scheme in Fig. 1.

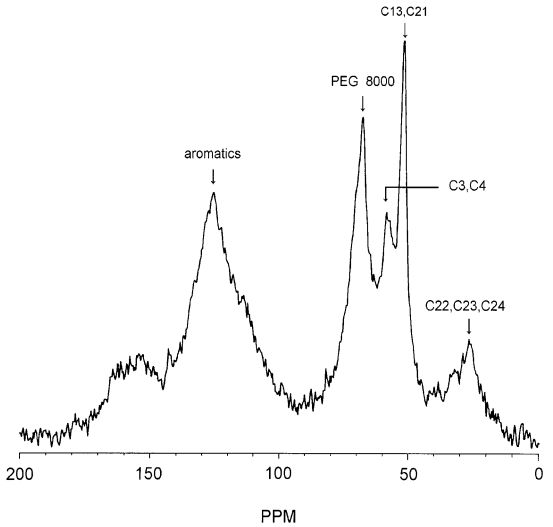

Fig. 9. The CPMAS ^{13}C-NMR spectrum of an intact capsule core from SCH 48461 capsule lot B (18 months at 30°C/60% RH). The NMR peak assignments correspond to the structure and atom numbering scheme in Fig. 1.

bon (–C–) peaks remain because it has no directly attached protons to rapidly dephase the ^{13}C signal. Methyl carbon ($-CH_3$) peaks remain because methyl groups are always in rapid motion at room temperature. In contrast, the cross-depolarized or interrupted decoupled ^{13}C-NMR spectrum of a plastic/waxy solid would be identical to the CPMAS spectrum. The result of the cross-depolarization experiment for lot C is shown in the bottom spectrum in Fig. 10. By comparing the top and bottom spectra in Fig. 10, the peaks associated with the methine (–CH–) and methylene ($-CH_2-$) carbons have completely disappeared and the remaining peaks are due to the six quaternary carbons (i.e., C2, C17, C9, C6, C14 and C25) and the two methyls (i.e., C13 and C21). Similar results for lot C were obtained with the interrupted decoupling experiment (not shown). The results of the cross-depolarization and interrupted decoupling experiments for the lot C samples are consistent only with the presence of crystalline SCH 48461 drug in the capsule PEG–drug solid dispersion matrix.

There are three other lines giving evidence supporting the presence of crystalline SCH 48461

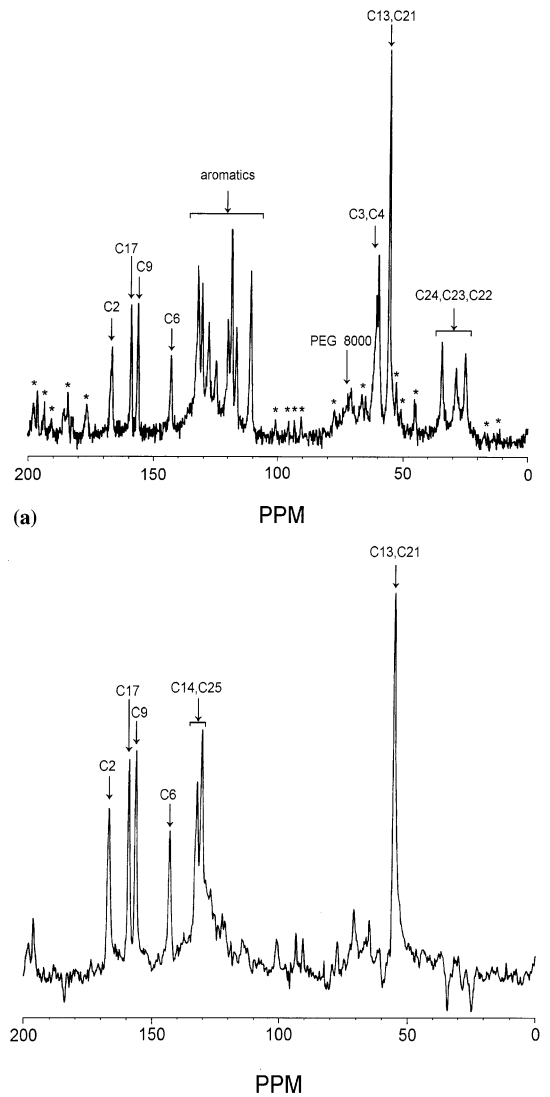

Fig. 10. The CPMAS ^{13}C-NMR spectrum (top spectrum) of an intact capsule core from SCH 48461 capsule lot C (24 months at room temperature) and its corresponding cross depolarization ^{13}C-NMR spectrum (bottom spectrum). The NMR peak assignments correspond to the structure and atom numbering scheme in Fig. 1. Chemical shift anisotropy of SCH 48461 is noted by the presence of significant rotational sidebands (marked by an asterisk). Cross-depolarization (CDP) experiments used a 40 μs phase inversion time and the phase of the ^{1}H spin lock changed by 180° at the end of the contact time.

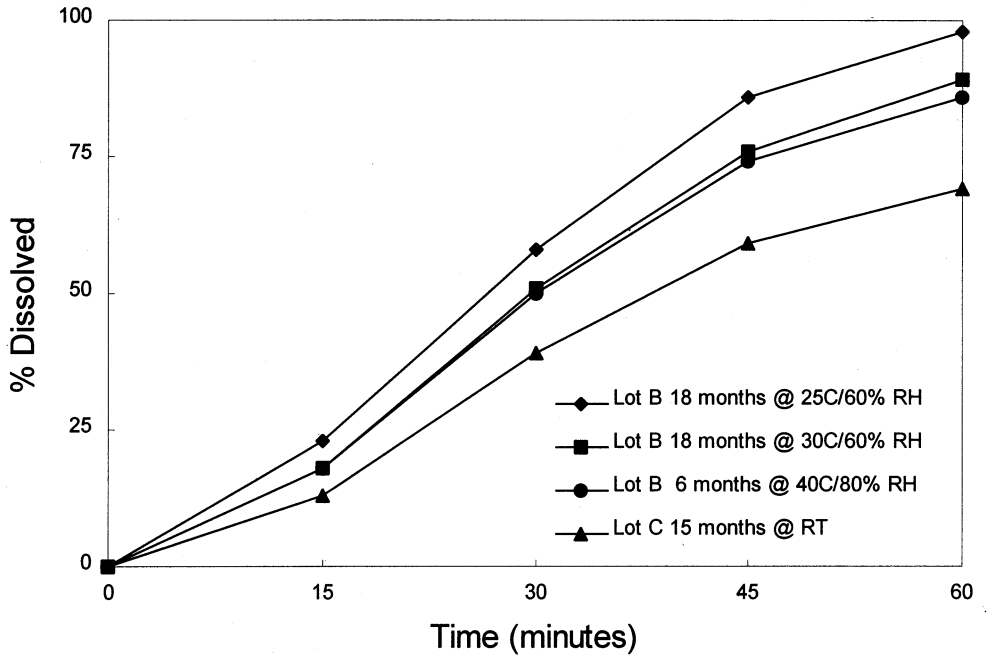

Fig. 11. The dissolution rate profiles of SCH 48461 capsule lot B (18 months at 25°C/60% RH, 18 months at 30°C/60% RH and 6 months at 40°C/80% RH) and lot C (15 months at room temperature).

drug in the lot C solid dispersion matrix. (1) The narrowest linewidths in the lot C spectrum are 35–50 Hz which are close to the 25 Hz linewidth for crystalline glycine. (2) The chemical shift anisotropy of SCH 48461, as evidenced by the presence of significant rotational sidebands (marked by an asterisk in the top spectrum of Fig. 10), would not be present if there were rapid molecular motion. (3) Crystalline solids cross-polarize (i.e., signal intensity builds up) more rapidly than do solids in which rapid molecular motion is present. The signal from the lot C samples built up rapidly, consistent with the presence of crystalline drug in the solid dispersion matrix.

The CPMAS spectra for lots A and B (Figs. 8 and 9) have several identifiable broad peaks. These spectra are consistent with that due to an amorphous material in which the SCH 48461 molecules are present in a variety of molecular environments. Other samples of lot B aged under different storage conditions (i.e., 6 months at 40°C, 18 months at 25H, and 18 months at 30H) gave spectra very similar to that shown in Fig. 9. It was noted that the intensity ratio of either the methoxy methyls (≈ 55 ppm) or the tallest aromatic peak (120–130 ppm) to the PEG 8000 methylenes (70 ppm) were much greater for the lot C spectra than any of the lot B spectra by a factor of approximately two. The magnitude of these ratios is probably indicative of the ease with which the drug molecules cross-polarize relative to PEG 8000. We assume that the cross-polarization rate for PEG 8000 does not change from sample to sample. An increase in the ratios may thus be indicative of an increase in the degree of crystallinity of the SCH 48461 drug in a particular solid dispersion sample matrix and a rank ordering of the SCH 48461 capsule lots based on their CPMAS ^{13}C-NMR spectral characteristics (i.e., relative peak ratios) was made. The amount of crystallinity increases from lot B (25°C/60% RH $\leqslant$ 30°C/60% RH $\leqslant$ 40°C/80% RH) $<$ lot C which is directly correlated to their respective dissolution profiles (Fig. 11).

4. Conclusions

ATR-IR microspectroscopic analysis of the SCH 48461 capsule lots indicated that lot A contained only amorphous drug and had no inter- and intra-capsule core IR spectral differences, lot C had very large inter- and intra-capsule core IR spectral differences, which were attributable to the presence of a crystalline drug fraction, and lot B had IR spectral characteristics somewhere in between that of lot A and lot C. Solid-state CPMAS ^{13}C-NMR analysis confirmed the presence of crystalline drug fraction in the problematic SCH 48461 capsule lots, and both ATR-IR and CPMAS ^{13}C-NMR spectral results produced a rank ordering of the crystalline drug fraction present in the SCH 48461 capsule lots that corresponded to the dissolution results.

The following conclusions can be made based on the results from dissolution, solid-state ATR-IR analysis, and solid-state CPMAS ^{13}C-NMR analysis of the SCH 48461 capsule lots. The reduction of the dissolution rate during the storage of SCH 48461 capsule lot B was caused by the formation of amorphous drug deposits in the drug–PEG solid dispersion matrix that gradually crystallized during storage. The incomplete dissolution of SCH 48461 capsule lot C was caused by the formation of amorphous/crystalline drug deposits in the drug–PEG solid dispersion matrix at the time of manufacture. These results are consistent with studies of griseofulvin–PEG and indomethacin–PEG solid dispersion systems [2,4,8,9].

Acknowledgements

The authors wish to thank Dr Herman Lock at Colorado State University Regional NMR Center for the preliminary ^{13}C-NMR spectral analysis, and Professor James E. Roberts at Lehigh University for the confirmatory ^{13}C-NMR spectral analysis and his interpretations of the spectra. The authors would also like to thank Charles Eckhart at Schering-Plough Research Institute in obtaining and interpreting the X-ray powder diffraction patterns.

References

[1] S. Byrn, Solid-State Chemistry of Drugs, Academic Press, New York, 1982.
[2] J. Ford, Pharm. Acta Helv. 61 (3) (1986) 69–88.
[3] J. Haleblian, J. Pharm. Sci. 64 (1975) 1269–1288.
[4] W. Chiou, S. Riegleman, J. Pharm. Sci. 60 (1971) 1281–1302.
[5] D. Burnett, Tetrahedron Lett. 35 (40) (1994) 7339–7342.
[6] D. Burnett, M. Caplen, H. Davis, R. Burrier, J. Clader, J. Med. Chem. 37 (12) (1994) 1733–1736.
[7] S. Walker, J. Ganley, K. Bedford, T. Eaves, J. Pharm. Pharmacol. 32 (1980) 389–393.
[8] J. Ford, M. Rubinstein, Pharm. Acta Helv. 54 (12) (1979) 353–358.
[9] W. Chiou, J. Pharm. Sci. 66 (1977) 989–991.
[10] H. Klug, L. Alexander, X-Ray Diffraction Procedures for Polycrystalline and Amorphous Materials, 2nd ed., Wiley-Interscience, New York, 1974.
[11] W. Kidd, P. Varlashkin, C. Li, Powder Diff. 8 (1993) 180–187.
[12] H. Brittain, K. Morris, D. Bugay, A. Thakur, A. Serajuddin, J. Pharm. Biomed. Anal. 11 (1993) 1063–1069.
[13] M. Kuhnert-Brandstatter, H. Sollinger, Mikrochim. Acta (Wein) III (1990) 233–258.
[14] R. Fletton, R. Harris, A. Kenwright, R. Lancaster, K. Packer, N. Sheppard, Spectrochim. Acta 43A (1987) 1111–1120.
[15] R. Harris, B. Say, R. Yeung, R. Fletton, R. Lancaster, Spectrochim. Acta 45A (1989) 465–469.
[16] B. Hegedus, S. Gorog, J. Pharm. Biomed. Anal. 3 (1985) 303–313.
[17] S. Paul, C. Schutte, Mikrochim. Acta (Wein) III (1988) 171–173.
[18] A. Tudor, S. Church, P. Hendra, M. Davies, C. Melia, Pharm. Res. 10 (1993) 1772–1776.
[19] A. Terol, A. Bouassab, B. Pauvert, P. Chevallet, G. Cassanas, Thermochim. Acta 225 (1993) 97–109.
[20] M. Block, G. Depke, U. Egner, A. Muller-Fahrnow, G. Winter, Tetrahedron 50 (1994) 13125–13134.
[21] R. Kellner, M. Kuhnert-Brandstatter, H. Malissa, Mikrochim. Acta (Wein) III (1988) 153–165.
[22] J. Reffner, Pract. Spectrosc. 6 (1988) 179–196.
[23] R.J. Markovich, Ph.D. Dissertation, Purdue University, West Lafayette, IN, 1990.
[24] J. Reffner, J. Coates, R. Messerschmidt, Am. Lab. April (1987) 86-97.
[25] J. Reffner, W. Wihlborg, Am. Lab. April (1990) 26-34.
[26] J. Katon, A. Sommer, Appl. Spectrosc. Rev. 25 (3–4) (1990) 173–211.
[27] Introduction to Attenuated Total Internal Reflectance (ATR) Spectroscopy, Spectra-Tech FT-IR Technical Note TN-1, Spectra-Tech, Stamford, CT.
[28] ATR Microscopy, Spectra-Tech Product Data Sheet PD-8, Spectra-Tech, Stamford, CT.
[29] A. Pines, M. Gibby, J. Waugh, J. Chem. Phys. 56 (1972) 1776–1777.

[30] A. Pines, M. Gibby, J. Waugh, Chem. Phys. Lett. 15 (1972) 373–376.
[31] A. Pines, M. Gibby, J. Waugh, J. Chem. Phys. 59 (1973) 569–590.
[32] A. Cholli, W. Ritchey, J. Koenig, W. Veeman, Spectrosc. Lett. 21 (1988) 519–531.
[33] S. Opella, M. Frey, J. Am. Chem. Soc. 101 (1979) 5854–5856.
[34] D. Bugay, Pharm. Res. 10 (1993) 317–327.